Semiflexible polymers grafted to a solid planar substrate: Changing the structure from polymer brush to "polymer bristle"

ARTICLE *in* THE JOURNAL OF CHEMICAL PHYSICS · MAY 2012

Impact Factor: 2.95 · DOI: 10.1063/1.4712138 · Source: PubMed

2 AUTHORS:

Andrey Milchev
Bulgarian Academy of Sciences
237 PUBLICATIONS **4,464** CITATIONS
SEE PROFILE

Kurt Binder
Johannes Gutenberg-Universität Mainz
1,065 PUBLICATIONS **45,258** CITATIONS
SEE PROFILE

Semiflexible polymers grafted to a solid planar substrate: Changing the structure from polymer brush to "polymer bristle"

A. Milchev and Kurt Binder

Citation: J. Chem. Phys. **136**, 194901 (2012); doi: 10.1063/1.4712138
View online: http://dx.doi.org/10.1063/1.4712138
View Table of Contents: http://jcp.aip.org/resource/1/JCPSA6/v136/i19
Published by the American Institute of Physics.

Semiflexible polymers grafted to a solid planar substrate: Changing the structure from polymer brush to "polymer bristle"

A. Milchev[1,2] and Kurt Binder[2]
[1]*Institute of Physical Chemistry, Bulgarian Academy of Sciences, 1113 Sofia, Bulgaria*
[2]*Institut für Physik, Johannes Gutenberg Universität Mainz, Staudinger Weg 7, 55099 Mainz, Germany*

(Received 6 March 2012; accepted 19 April 2012; published online 15 May 2012)

Monte Carlo simulations are presented for a coarse-grained model of polymer brushes with polymers having a varying degree of stiffness. Both linear chains and ring polymers grafted to a flat structureless non-adsorbing substrate surface are considered. Applying good solvent conditions, it is shown that with growing polymer stiffness the brush height increases significantly. The monomer density profiles for the case of ring polymers (chain length $N_R = 64$) are very similar to the case of corresponding linear chains ($N_L = 32$, grafting density larger by a factor of two) in the case of flexible polymers, while slight differences appear with increasing stiffness. Evidence is obtained that the chain dynamics in brushes is slowed down dramatically with increasing stiffness. Very short stiff rings ($N_R \leq 16$) behave like disks, grafted to the substrate such that the vector, perpendicular to the disk plane, is oriented parallel to the substrate surface. It is suggested that such systems can undergo phase transitions to states with liquid crystalline order. © *2012 American Institute of Physics*. [http://dx.doi.org/10.1063/1.4712138]

I. INTRODUCTION

Polymer brushes are obtained by grafting macromolecules via special chemical groups to a (non-adsorbing) solid substrate surface (see Refs. 1–10 for reviews). Due to the delicate interplay between configurational entropy of these (flexible) polymers, excluded volume, and (solvent mediated) enthalpic interactions, the structure of these soft polymeric layers and their response to external perturbations is characterized by very diverse, complex, and rich properties. Despite the fact that polymer brushes are used for various applications,[8] there are still aspects of the complex behavior of such systems that are not yet well understood, and more research still is needed to clarify them.

The aspect of polymer brush behavior on which we focus here is the fact that many polymers of interest exhibit significant chain stiffness, in particular many biopolymers of interest are "semiflexible,"[11] and their "persistence length"[12] that characterizes their stiffness can vary to a great extent. One can show that a DNA, for example, can facilitate barrier crossing[13] by stretching during transport across membranes. Already the conformation and pulling-force response of an isolated (long) semiflexible polymer in solution under good solvent conditions shows a very rich behavior, with several distinct scaling regimes (see Ref. 14 for a review). At higher concentrations solutions of semiflexible polymers may exhibit liquid crystalline order,[15,16] and this ordering may be enhanced by confining walls.[17] Grafting short semiflexible polymers to a substrate at high grafting density, the resulting brush is expected to be less soft and therefore is called "bristle" (e.g., Ref. 18). Expectedly, the impact of semiflexibility on the properties of polymer brushes is most frequently observed in polyelectrolyte and polyampholyte brushes.[19,20] There have been several theoretical[21,22] and simulational[23] studies of semiflexible polymer brushes and their behavior at varying solvent quality,[24,25] or in shear flow,[26] whereby good agreement with experiments has been observed. Nonetheless, the properties of such systems have received relatively much less attention than brushes formed from flexible polymers (with the notable exception of the case of poor solvent conditions, where various types of micellar structures were predicted to form[30]). The latter applies even more so to brushes formed by grafting ring polymers to a flat surface although there have been several studies of looped brushes.[27–29] Also the relaxation behavior of semiflexible grafted polymers has found little attention, apart from a recent interesting study of a single grafted polymer.[31]

In the present paper, we contribute to fill this gap, studying the effect of variable polymer stiffness for polymer brushes under good solvent conditions, focusing on both grafted linear polymers (with length $N_L = 32$ at grafting density σ_g) and ring polymers of length $N_R = 2N_L$ and grafting density $\sigma_g/2$. Section II defines the model and the simulation method, Sec. III describes the results on the density profiles (including also the distributions of the chain ends), and eventually focuses on the liquid-crystalline order that is detected for grafted stiff ring polymers, which is reminiscent of the ordering behavior of discotic molecules (see, e.g., Ref. 32) in thin film geometry (see, e.g., Refs. 33–35). Section IV summarizes our conclusions.

II. MODEL AND SIMULATION METHOD

We study off-lattice coarse-grained models of polymers, where beads are connected by (anharmonic) springs described by a finitely extensible nonlinear elastic (FENE) potential defined as

$$U_{\mathrm{FENE}}(\ell) = U_0 \ln[1 - (\ell - \ell_0)^2/(\ell_0 - \ell_{\max})^2], \qquad (1)$$

where ℓ is the length of a bond connecting two neighboring monomers, which can vary between $\ell_{\min} < \ell < \ell_{\max}$, where $\ell_{\max} = 1$ is chosen as our unit of length, $\ell_{\min} = 0.4$, the energetically preferred bond length then being $\ell_0 = 0.7$, and the constant U_0 is chosen as $U_0 = 20$.

The stiffness of the polymers is controlled by a bond bending potential $V_b(\theta)$, where θ is the angle between subsequent bonds, and is chosen as

$$V_b(\theta) = f\theta^2. \tag{2}$$

Note that for small angles θ this potential is identical to the choice $V_b(\theta) = 2f(1 - \cos\theta)$ frequently encountered in the literature (e.g., Ref. 17). One should mention that potentials of the type of Eqs. (1) and (2), can be justified by systematic coarse-graining procedures where several carbon-carbon bonds along the backbone of a polymer are lumped into effective bonds connecting effective monomeric units, see e.g., Refs. 36 and 37. The case $f = 0$ corresponds to fully flexible polymers, that were extensively studied before (e.g., Ref. 38). It turns out that for our model the suitable range of the constant f to be studied is $0 \le f/k_BT \le 3$ (here, $k_B \equiv 1$ denotes Boltzmann's constant, and T is the absolute temperature). Finally, the interaction between non-bonded monomers is described by a Morse potential[38–41]

$$U_M(r) = \varepsilon\{\exp[-2\alpha(r - r_{\min})] - 2\exp[-\alpha(r - r_{\min})]\} \tag{3}$$

with parameters $\varepsilon = 1$, $r_{\min} = 0.8$, and $\alpha = 24$. Due to the attractive character of this potential at small distances, under dilute solution conditions for $N \to \infty$ a well defined theta point occurs, which has been estimated to be $k_BT/\varepsilon = 0.62$.[40] Here, we use $k_BT/\varepsilon = 1$, i.e., the system is in the good solvent regime. We use the standard Monte Carlo algorithm[41] where one randomly chooses single monomers and attempts to displace them to a new position in their environment, $\vec{r}_i\,' = \vec{r}_i + \Delta\vec{r}$. The displacement $\Delta\vec{r}$ is randomly chosen from a cube of linear dimension δ centered at the old position, with $\delta = 0.25$. For $f = 0$ this algorithm executes rather fast, due to the short range of the Morse potential only a few neighbors need to be checked to compute the energy change associated with a move.

Most of the Monte Carlo simulations were carried out with chain length $N = N_L = 32$ of linear polymers at grafting density $\sigma_g = 0.125$, and for a system of ring polymers with $N_R = 64$ but $\sigma_g = 0.0625$ (so that each ring polymer corresponds to two linear polymers in the ordinary brush, i.e., the total number of effective monomers in both systems is the same). We choose a substrate of linear dimensions $L \times L$, oriented perpendicular to the z-direction, and apply periodic boundary conditions in x- and y-directions, choosing $L = 32$, i.e., the system contains $N_{ch} = 128$ chains (4096 monomers). This choice of lateral linear dimensions is sufficiently large as long as the brush stays in a disordered state. Typical configurations of such disordered brushes are shown in Fig. 1. One can see that the increase of f leads to a significant stiffening of the chains and a related strong increase of the brush height. However, for $f = 3$ the problem of equilibrium becomes very delicate. This is seen when the autocorrelation functions of

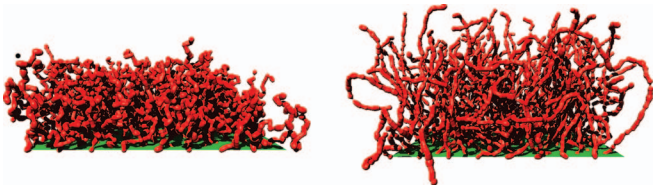

FIG. 1. Snapshots of a polymer brush of linear chains with chain length $N = 32$ and grafting density $\sigma_g = 0.125$, for fully flexible chains (bending stiffness constant $f = 0$ (left)) and semiflexible chains with $f = 3.0$ (right). The substrate surface is a hard wall, linear dimension L of the $L \times L$ surface is $L = 32$, so the total number of chains included is $N_{ch} = 128$.

the squared end-to-end distance are examined,

$$C^{\perp}_{R_e^2}(t) = \frac{\langle (R_e^z(t))^2 (R_e^z(0))^2\rangle - \langle (R_e^z)^2\rangle^2}{\langle (R_e^z)^4\rangle - \langle (R_e^z)^2\rangle^2} \tag{4}$$

and

$$C^{||}_{R_e^2}(t) = \frac{\langle (R_e^x(t))^2 (R_e^x(0))^2\rangle - \langle (R_e^x)^2\rangle^2}{\langle (R_e^x)^4\rangle - \langle (R_e^x)^2\rangle^2}. \tag{5}$$

Only when relaxation functions $C(t)$ (for simplicity we omit here sub- and superscripts) have been followed over sufficiently long time t so that $C(t) \approx 0.1$, can one assume that[47] $C(t) \propto \exp(-t/\tau)$. By fitting $C(t)$ to an exponential decay in the region from about $C(t) \approx 0.2$ to about $C(t) \approx 0.05$, we have estimated the relaxation times shown in Fig. 2(c).

Figure 2 shows that for flexible chains ($f = 0$) a time of 10^5 Monte Carlo steps (MCS) per bead suffices that these functions decay to less than about 0.1, so that equilibrium properties can be reliably estimated with runs of a length of about a million MCS. For stiff chains ($f = 3.0$), on the other hand, the figure indicates that then runs are necessary that are at least an order of magnitude longer. Note that in the case of ring polymers, containing N_R monomers per ring, we reinterpret $\vec{R}_e$ as the vector connecting the grafting site (next to the monomer $i = 1$ of the ring polymer) to the monomer $i = N_R/2$, the "middle monomer" of the ring. The initial configuration of the ring polymers is constructed such that no pair of "catenated" (i.e., permanently entangled) loops occurs. Since the dynamics of our random hopping algorithm involving strictly local moves forbids any chain crossing, it also cannot happen that catenation occurs in the course of the simulation. It is interesting to note that for $f/k_BT \le 2$ all relaxation times are almost the same for parallel and perpendicular components of R_e and there is no difference between linear chains and rings. Only for $f/k_BT \ge 2$ the rings start to get significantly slower than the corresponding linear chains.

III. RESULTS

We begin our discussion by presenting the profiles $\phi(z)$ of the total monomer density (Fig. 3(a)) and of the density distribution of the chain ends, $\rho(z)$, Fig. 3(b). One can see the typical features of $\phi(z)$, familiar from previous simulations of polymer brushes formed from fully flexible chains:[3,5,6,9,10] Near $z = 0$ there occurs an oscillation of $\phi(z)$, which is

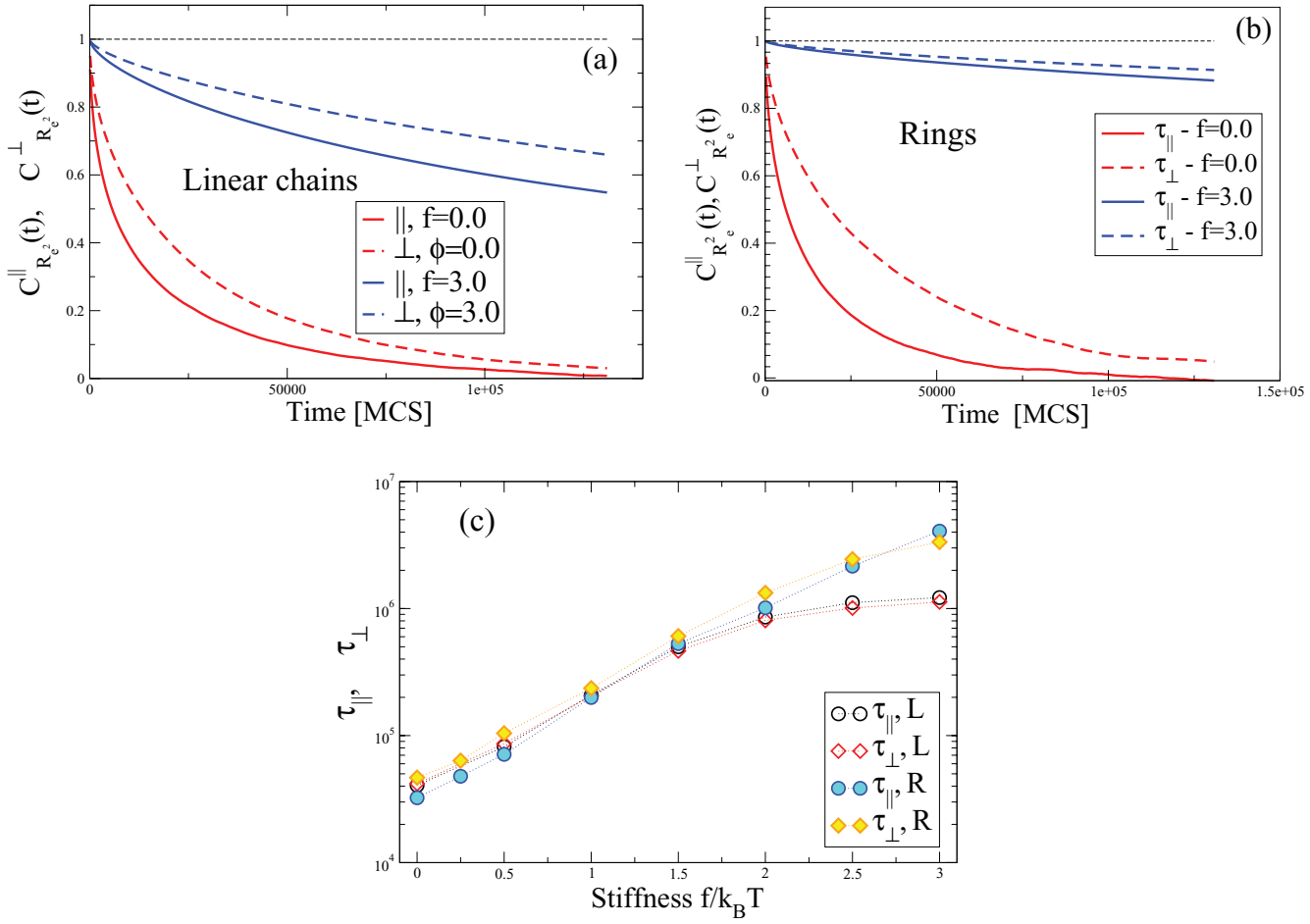

FIG. 2. Correlation functions $C^{||}_{R_e^2}(t)$ and $C^{\perp}_{R_e^2}(t)$, as defined in Eqs. (4) and (5), plotted versus time t (in the time units of attempted moves per monomer, MCS). (a) The case of linear chains with $N = 32$, $\sigma = 0.125$, comparing data for $f = 0$ with data for $f = 3$ and (b) data for grafted rings $f = 0.0$, 3.0. (c) The variation of relaxation times parallel $\tau_{||}(f)$ and perpendicular $\tau_{\perp}(f)$ to grafting plane with stiffness f for linear (L) and ring (R) polymer brush with $N_L = 32, N_R = 64$ at equivalent grafting density, $\sigma_g = 0.125, 0.0625$, cf. text.

attributed to a "layering effect" (like in the packing of hard spherical particles at a repulsive wall), see e.g., Ref. 42 for corresponding simulations. At somewhat larger distances from the wall $\phi(z)$ is essentially flat and crosses over to an (almost) parabolic decay, which does not extend to $\phi(z = h) = 0$ at the brush height h, however, but rather $\phi(z)$ exhibits an inflection point and thereafter a gradual decay in a tail of the profile occurs, extending to values of z much larger than the brush height h. We define the latter as usual from the first moment of the profile

$$h = (8/3) \int_0^\infty \phi(z) z dz / \int_0^\infty \phi(z) dz, \tag{6}$$

recalling that the prefactor 8/3 is chosen such that it agrees with the definition of h for the parabolic profile, $\varphi(z) \propto (1 - z^2/h^2)$.[1–3] On the other hand, the distribution of the chain ends $\rho(z)$ and of the z-components of the gyration radius $\rho(R_{gz})$ retain their general characteristics irrespective of chain stiffness: the density $\rho(z)$ of chains ends stays nonzero even for $z \to 0$, i.e., chain ends occur everywhere in the brush, not only near $z = h$; and $\rho(R_{gz})$ is zero near $R_{gz} = 0$ (which means, configurations where all the monomers are adsorbed at the repulsive wall never occur, of course), but then $P(R_{gz})$ rises to reach a shoulder at less than one half the value, where the peak of $P(R_{gz})$ occurs. The inset of Fig. 3(a) shows that h first increases linearly with f and then levels off: Of course, already for $f = 0$ we have $h \propto N$ for a polymer brush (disregarding the regime of "polymer mushrooms"[2,10] here), and the maximum extension (reached only for $f \to \infty$) would be $h = \ell_{\max} N$, if all chains are stretched out like rigid rods. It is interesting to note, however, that the range of the layering effect (density oscillations in $\phi(z)$) also increases with increasing f, in spite of the fact that $\phi(z)$ decreases for the values of z where the layering occurs. This is opposite to the behavior of simple liquids near hard walls where the range of layering increases with growing density.[42] One can understand this by noting that the observed layering effect is not caused by excluded volume interactions between particles as in the case of simple liquids but rather by stronger ordering and localization of the monomer positions along the semiflexible backbone of the brush polymers as the stiffness f gradually grows. In some sense, the transformation of a soft polymer brush into a bristle of strings creates an ordered array of monomers in the vicinity of the grafting plane.

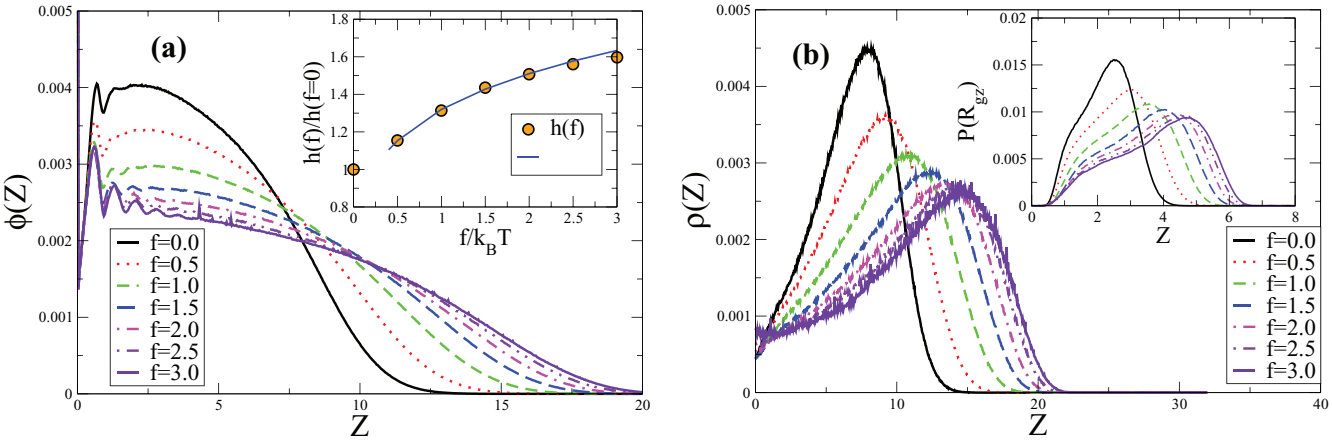

FIG. 3. (a) Density distribution of the monomer density $\phi(z)$ in the polymer brush with linear chains for $N = 32$, $\sigma = 0.125$, as function of the distance z from the grafting plane, including various choices of the bending stiffness f, as indicated. Inset shows the relative increase of the brush height $h(f)/h(0)$ versus f/k_BT. Line is used as guide to the eye only. (b) Density distribution of the free chain ends $\rho(z)$ in the polymer brush with $N = 32$, $\sigma_g = 0.125$ as a function of the distance z from the grafting plane, including various choices of the bending stiffness f, as indicated. Inset displays corresponding probability distributions of the z-component R_gz of the gyration radius of brush polymers.

Figure 4 presents the comparison with analogous quantities for ring polymers, choosing $N_R = 2N_L = 64$ but $\sigma_g = 1/16 = 0.0625$, such that each ring is equivalent to two linear chains. This picture suggests to compare the distribution function of the "middle monomer" ($i = N_R/2 = 32$, if monomers are labeled consecutively $i = 1, 2, \ldots$, starting at the grafted monomer) with the end monomer distribution of the linear chains. Recall that we have prepared the initial configuration of the ring polymers without any "catenation" (permanent entanglement) between different ring polymers. While for $f = 0$ the monomer density profile for linear polymer brushes and corresponding ring polymer brushes are almost identical (as pointed out in our recent earlier work[38]), for large f we do see some significant differences: there is no layering in $\phi(z)$ for ring polymers beyond the first peak, unlike the case of linear polymers. These differences are more clearly recognized when corresponding distributions are superposed (Fig. 4). It is remarkable, that $\rho(z \to 0) = 0$ for the rings, while $\rho(z \to 0) > 0$ for the corresponding linear chains.

A local measure of stretching is the average angle $\langle\theta\rangle$ between subsequent bonds, which shows a monotonous decrease with increasing f (Fig. 5), to $\Theta \approx 30^\circ$ for both linear chains and rings. Remarkably, it appears that the increased topological connectivity of the cyclic chains has little impact on the mean bending angle Θ even at very high degree of stiffness f. If one would consider a grafted and strongly stretched ring polymer as equivalent to two grafted and strongly stretched linear polymers, jointed at their otherwise free chain ends, one might expect a large angle $\langle\theta_i\rangle$ for monomers i near $N_R/2$. However, this does not seem to be the case. Evidently, in order to minimize the free energy, ring polymers compromise the complete folding ($\Theta \approx 180^\circ$) of two successive bonds onto one another while keeping the remaining angles small enough. The energy first increases with increasing f/k_BT, it reaches a maximum at about $f/k_BT \approx 1$, and then decreases somewhat before reaching a plateau value at large f. Note that this plateau of the potential energy is of the order $k_BT/2$: thus there is no significant energy gain possible

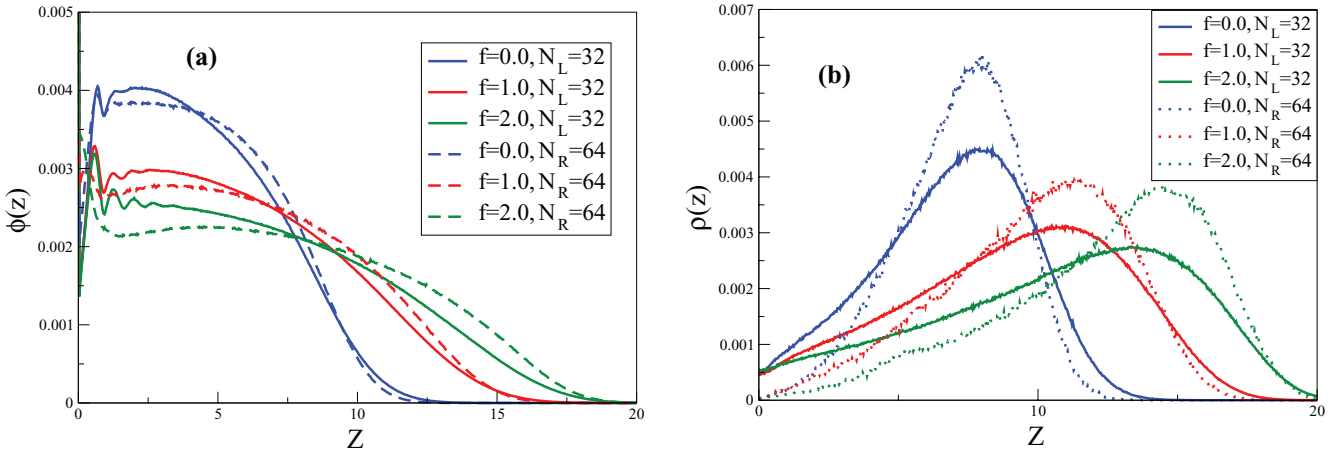

FIG. 4. (a) Comparison of density profiles $\phi(z)$ of monomers in brushes formed from linear chains (full curves) and from the corresponding ring polymer (broken curves). Three cases $f = 0$, 1, 2 are included, as indicated. (b) Same as (a), but distribution of end monomers (of linear chains) compared to the distributions of the corresponding middle monomers of rings.

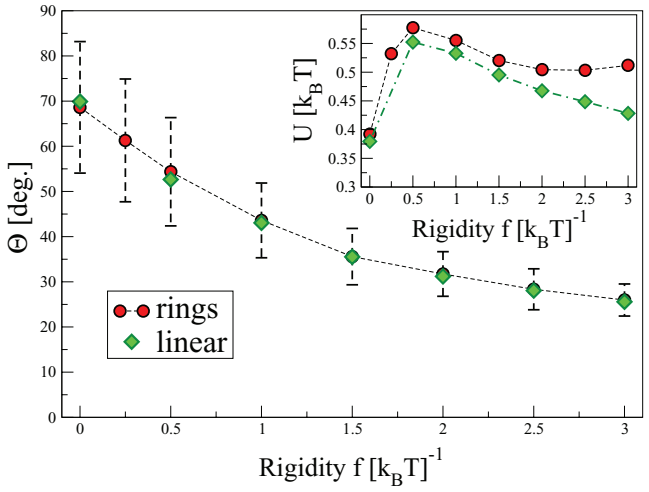

FIG. 5. Plot of the average angle $\langle\theta\rangle$ between subsequent bonds, averaged over all bonds in a polymer, plotted against the rigidity parameter f/k_BT, for both linear chains and ring polymers. Note that in the plot of $\langle\theta\rangle$ vs. f the symbols for rings and linear chains coincide precisely for $f/k_BT \geq 1$, although the corresponding internal energies do not! Inset shows the corresponding variations of the internal energy. All data are for $N = 32$, $\sigma = 0.125$ (linear chains) or $N_R = 64$, $\sigma = 0.0625$ (rings), respectively.

by reducing the typical angle $\langle\theta\rangle$ (which still is of the order of 30° for $f/k_BT = 3.0$) further. The minimal energy in our model thus involves a significant entropic contribution due to orientational disorder of the bonds of the chain.

The gradual decrease of $\langle\theta\rangle$ with increasing f/k_BT (Fig. 5) is accompanied by a gradual increase of the chain linear dimensions (Fig. 6). While it is expected from the increase of brush height (Figs. 3 and 4) with f/k_BT that the components of the polymer radii perpendicular to the grafting surface must increase, the fact that the parallel components also increase as well at first sight is unexpected. From the decrease of $\langle\theta\rangle$ with f/k_BT one could expect that the monomers of a chain are less spread out in lateral direction, and occur only over smaller distances from the grafting sites, in the directions parallel to the substrate when f/k_BT is large. This obviously is not the case! We interpret this surprising finding that the stronger stretching goes along with a reduction of the average density of the brush (Figs. 3 and 4), which enables larger fluctuations in the chain conformation, which then leads to large lateral components of the polymer radii. In the inset to Fig. 6(b) one can indeed verify that for linear semiflexible chains the probability distribution function of $R_{g||}$ broadens considerably with increasing rigidity f. A closer inspection of Figs. 6(a) and 6(b) reveals moreover that both $R^2_{e\perp}$ and $R^2_{g\perp}$ for a ring brush at any degree of rigidity f are larger than the respective vertical components for linear semiflexible chains. In contrast, as seen from the comparison of the parallel components in Figs. 6(a) and 6(b), for linear chains $R^2_{e||}$ is larger than for rings, while the opposite holds for $R^2_{g||}$. One can interpret this complex and unexpected behavior tentatively as due to the fact that the gyration ellipsoids of linear chains, i.e.,"cigars," are more extended as the stiffness is increased and attain thereby greater rotational freedom in the sense that they can precess about the surface normal more freely. On the contrary, grafted rings transform progressively into circles whereby their $R^2_{g||}$ grow with f, exceeding the respective $R^2_{g||}$ of linear chains.

The above arguments apply if we consider relatively small and stiff polymers, containing just a few Kuhn segments. If, on the contrary, the number n_K of Kuhn segments is large enough, so that for $\langle R^2_{e||}\rangle$ Gaussian statistics in the semi-dilute regime applies, we conclude that $\langle R^2_{e||}\rangle \propto n_K l_K^2 = l_K N l_0$, where we recall that the contour length $Nl_0 = n_K l_K$, l_K being the length of the Kuhn segment. This argument shows that also the parallel linear dimension increases with l_K (and with increasing stiffness f).

Finally, we ask the question whether the interaction, Eq. (2), can lead to some nontrivial orientational order. Note that in all dense polymer brushes the chains are stretched in the direction perpendicular to the substrate, and since $R_{e,\perp} \propto N$, the bonds trivially exhibit some degree of nematic order with the "director" oriented in the z-direction, but this is of less interest in the present context, since this order develops gradually as the grafting density of the polymers at the surface increases, there is no transition where this type of

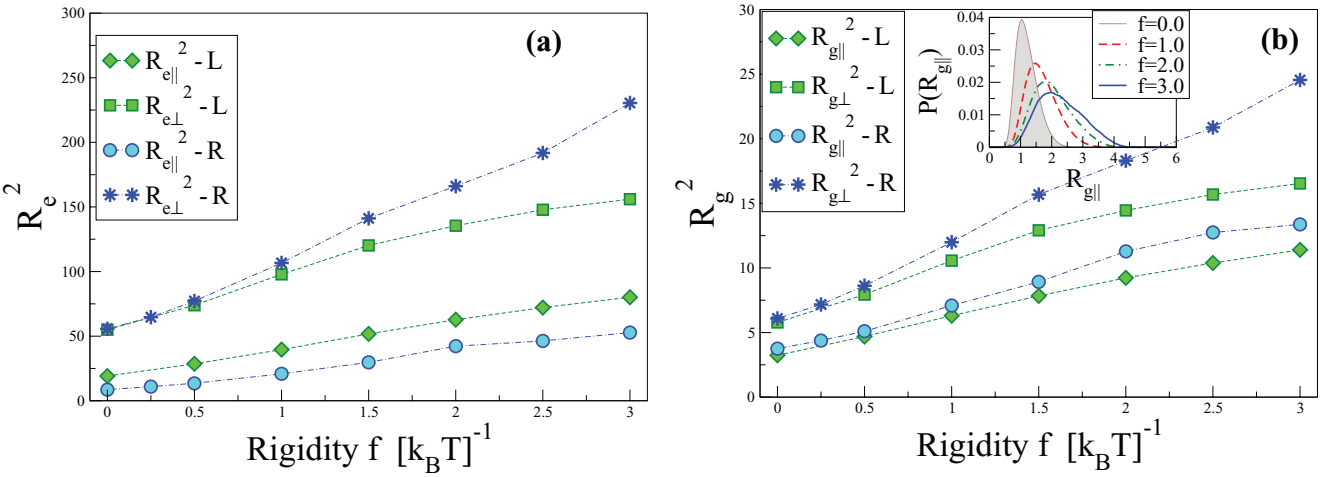

FIG. 6. Parallel and perpendicular linear dimensions of mean-squared end-to-end vector, R^2_e, (a), and of gyration radius, R^2_g, (b), of linear and ring polymers, plotted vs. f/k_BT, for the case $N = 32$, $\sigma = 0.125$ (linear chains) or $N_R = 64$, $\sigma = 0.0625$ (ring polymers), respectively.

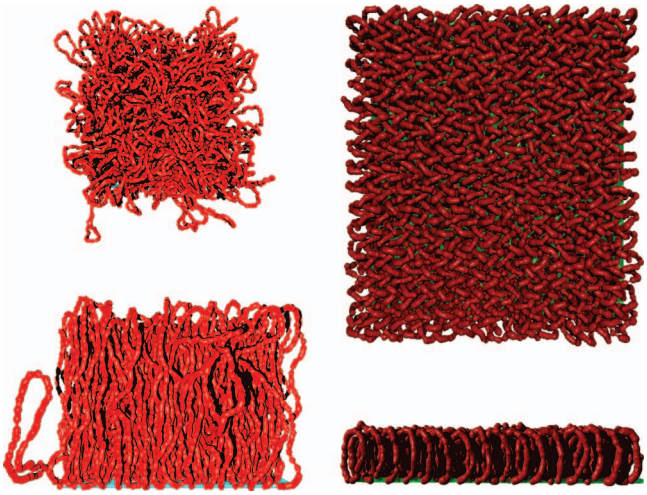

FIG. 7. Top view (above) and side view (below) of snapshot pictures of a polymer brush of ring length $N = 64, \sigma_g = 0.25$, $f/k_BT = 3.0$ (a) and $N = 16$, $\sigma_g = 0.5$, $f/k_BT = 3.0$ (b).

order appears abruptly, and no spontaneous symmetry breaking occurs.

The situation is different, however, when we consider densely grafted short ring polymers (Fig. 7). The shape of these short rings roughly is donut-like, if we associate to each ring the three eigenvectors of the gyration tensor, $\mathbf{R}_g^2(\mathbf{i}, \mathbf{j}) \to \vec{\mathbf{e}} = (\vec{e}_1, \vec{e}_2, \vec{e}_3)$. One typically has one eigenvector perpendicular to the grafting surface, one vector in the plane containing the grafting point and oriented along the long direction of the donut parallel to the grafting plane, while the third eigenvector is also parallel to the grafting plane but along the short direction of the "donut" (through its hole). These gyration tensor eigenvectors that are oriented parallel to the grafting plane are randomly oriented at low grafting density, but acquire long-range orientational order at high grafting densities, as the snapshots suggest (Fig. 7). So a nontrivial order-disorder transition is observed.

We may take the components of this eigenvector, pointing perpendicular to the disk-like molecules, as an order parameter and thus produce a snapshot picture of the ordering, disregarding the detailed information on the positions of the individual monomers (Fig. 8). Note that snapshots (b) and (c) are taken on both sides of the order-disorder transition that has been, very roughly, located to occur at $f = f_c \approx 1.7 k_BT$ (Fig. 9). The order parameter is a linear combination of angle orientations $\phi_{i,j}$ on a "plaquette" (or, unit cell) of 4 adjacent sites i, j on the grafting plane whereby ϕ is defined as

$$\tan \phi_{i,j} = \frac{e_{3y}(i, j)}{e_{3x}(i, j)} \tag{7}$$

and the order parameter itself is $\psi = |\phi_{i,j} + \phi_{i,j+1} - \phi_{i+1,j} - \phi_{i+1,j+1}|$.

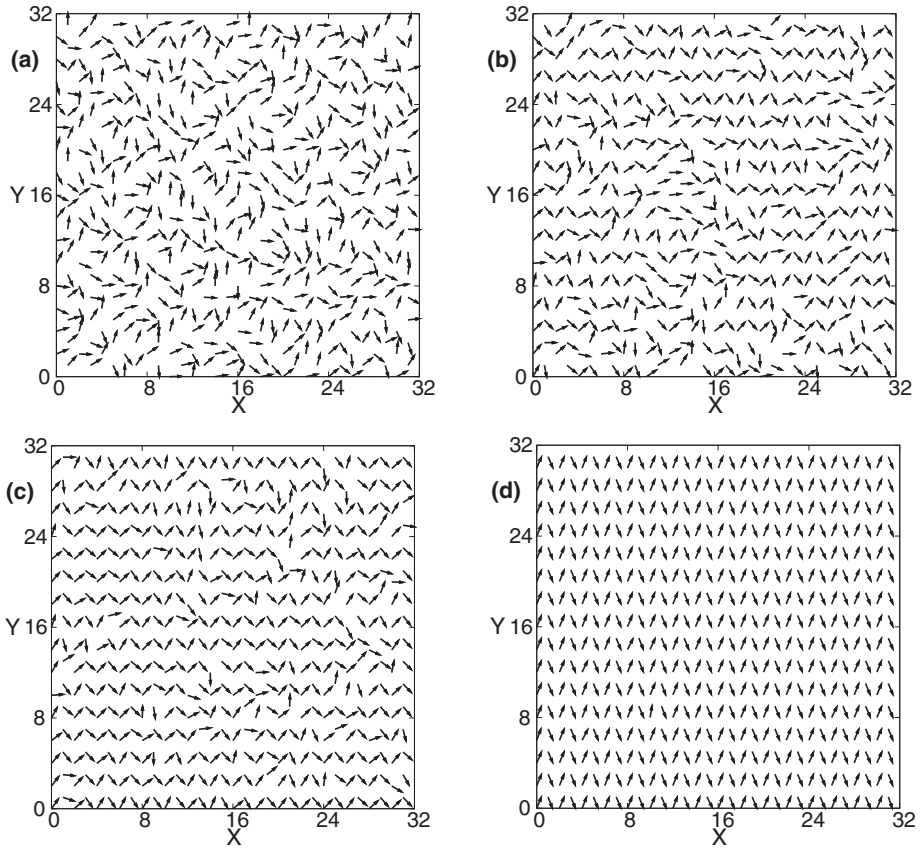

FIG. 8. Snapshot configurations of the unit vectors $\vec{e}_{i\perp}$ oriented along the projections of the eigenvectors corresponding to the smallest eigenvalue of each disk-like ring polymer in a brush with $N = 16$, $\sigma_g = 0.50$ into the grafting plane. As origin for each vector the grafting of the ring polymer is chosen (and these grafting sites are arranged according to a regular square lattice). Four choices of f/k_BT are included, namely, 0.0 (a), 1.5, 1.75, and 3.0 (clockwise). A lattice of 32×32 grafting sites is chosen, and periodic boundary conditions in the lateral direction parallel to the grafting plane are used.

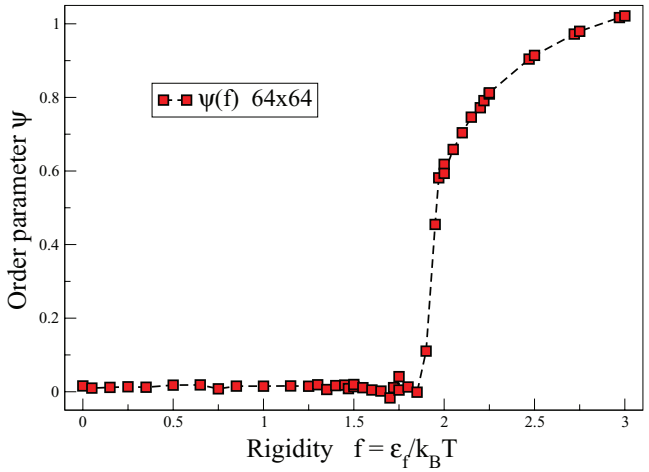

FIG. 9. Variation of the order-parameter ψ of the system shown in Fig. 8 plotted vs. f/k_BT.

Note that a careful finite size scaling analysis would be needed to clarify whether this transition is continuous or of first order; this must be left to future work, however. We also note that in real polymer brushes the grafting sites are arranged at random rather than regularly: this randomness likely will disturb the long-range order significantly. The situation is reminiscent of mesophase ordering in two-component (A, B) polymer brushes where the order-parameter components can be described as a wave-like pattern of the local relative concentration, $c(x) \propto \cos(\pi x/\lambda + \alpha)$, where λ is the wavelength characterizing the periodicity of the pattern, and α denotes the phase shift.[43] The randomness of the positions of the grafting sites is believed to act as a random field on such an order and hence only short-range order rather than long-range order is possible.[44–46] We expect similar problems here.

IV. CONCLUSIONS

In this paper, the effects of chain stiffness on the conformation of polymers in brushes are studied by Monte Carlo simulations, considering coarse-grained models of both brushes formed from linear chains and brushes formed of ring polymers grafted to a flat planar repulsive substrate. In both cases the increase of chain stiffness leads to an increase of brush height and a concomitant reduction of the monomer density in the region of the brush near the grafting surface. Despite this density decrease, the layering (density oscillations near the grafting wall) extends over a larger range for stiffer (linear rather than cyclic) chains. Regarding the question as to why this effect occurs only for linear chains and not for ring polymers, we see this as a manifestation of the increased degree of ordering in the linear brush with growing stiffness f whereby the chains attain a string-like structure leading to lattice-like positioning of the monomers in the vicinity of the grafting plane. In contrast, with increasing f the ring polymers expand laterally, trying to form disks whereby the distance of the monomers placed symmetrically with respect to the grafted monomer, i and $N - i$, regarding the consecutive number i along the ring backbone becomes progressively unequal.

Another interesting distinction between chains and ring polymers is that the density of chain ends remains nonzero near the grafting plane while the density of the "middle monomer" $i = N_R/2$ of ring polymers vanishes there (we choose the number of monomers per ring N_R always twice the number of beads N in the linear chains, and the grafting density is half that of the linear chains, so the number of monomers in both systems is strictly the same). On the other hand, the variation of the average angle $\langle\theta\rangle$ between consecutive bonds with the stiffness parameter f/k_BT for linear chains and rings is identical. Another counterintuitive effect is that the lateral chains dimensions (parallel to the grafting surface) also increase with f/k_BT, in addition to the extension of the polymers in the z-direction normal to the surface. Also the variation of chain linear dimensions with grafting density shows some unexpected features (Fig. 6(c)). All these findings show that the conformational organization of macromolecules in brushes contains many subtle features depending on the chain architecture, and a more microscopic analytic theory of these effects is called for.

We have also seen that the relaxation of the polymers gets much slower with increasing stiffness, particularly in the case of ring polymers. This fact severely hampers the detailed investigation of the novel order-disorder transition that we have discovered for short stiff rings. These rings attain the shape of almost elliptic rather than circular "donuts," and the eigenvectors of the smallest component of their gyration tensor (which is oriented perpendicular to the midplane of the "donut" and is parallel to the grafting surface), exhibit long-range orientational order similar to layers in discotic liquid crystal phases. However, we argue that this long-range order is facilitated by the checkerboard regular arrangement of grafting sites (on the sites of a square lattice) chosen in our model (for disordered brushes this regular arrangement has only negligible effects, in comparison to the more realistic choice of randomly distributed grafting sites). Thus, we have argued that for a random distribution of grafting sites only ordered domains having finite size can be expected. As far as a considerable computational effort would be required to study this problem in more detail, clarification of these issues must be left to further work. We hope that our study will motivate other experimentalists to study brushes formed from semiflexible polymers in more detail.

ACKNOWLEDGMENTS

This work was supported in part by the Deutsche Forschungsgemeinschaft (DFG) Grant No. B1314/23. We thank D. Reith and P. Virnau for useful discussions.

[1] S. Milner, Science **251**, 905 (1991).
[2] A. Halperin, M. Tirrell, and T. P. Lodge, Adv. Polym. Sci. **100**, 31 (1992).
[3] G. S. Grest and M. Murat, in *Monte Carlo and Molecular Dynamics Simulations in Polymer Science*, edited by K. Binder (Oxford University Press, New York, 1995), p. 476.
[4] J. Klein, Annu. Rev. Mater. Sci. **26**, 581 (1996).
[5] I. Szleifer and M. A. Carignano, Adv. Chem. Phys. **94**, 165 (1996).
[6] G. S. Grest, Adv. Polym. Sci. **138**, 149 (1999).
[7] L. Leger, E. Raphael, and H. Hervet, Adv. Polym. Sci. **138**, 185 (1999).
[8] *Polymer Brushes*, edited by R. C. Advincula, W. J. Brittain, K. C. Caster, and J. Rühe (Wiley VCH, Weinheim, 2004).

[9]R. Descas, J.-U. Sommer, and A. Blumen, Macromol. Theory Simul. **17**, 429 (2008).
[10]K. Binder, T. Kreer, and A. Milchev, Soft Matter **7**, 7159 (2011).
[11]T. Sanchez, I. M. Kulic, and Z. Dogic, Phys. Rev. Lett. **104**, 098103 (2010).
[12]A. Yu. Grosberg and A. R. Khokhlov, *Statistical Physics of Macromolecules* (AIP, New York, 1994).
[13]K. Lee and W. Sung, Phys. Rev. E **64**, 041801 (2001).
[14]H.-P. Hsu and K. Binder, J. Chem. Phys. **136**, 024901 (2012).
[15]A. N. Semenov and A. R. Khokhlov, Sov. Phys. Usp. **31**, 988 (1988).
[16]*Liquid Crystallinity in Polymers: Principles and Fundamental Properties*, edited by A. Ciferri (VCH, New York, 1991).
[17]V. A. Ivanov, A. S. Rodionova, E. A. An, J. A. Martemyanova, M. R. Stukan, M. Müller, W. Paul, and K. Binder, Phys. Rev. E **84**, 041810 (2011).
[18]A. Gopinath and L. Mahadevan, Proc. R. Soc. London, Ser. A (in press).
[19]M. Baratlo and H. Fazli, Eur. Phys. J. E **29**, 131 (2009).
[20]Q. Cao, C. Zuo, L. Li, and G. Yan, Biomicrofluidics **5**, 044119 (2011).
[21]M. Carignano and I. Szleifer, J. Chem. Phys. **98**, 5006 (1993).
[22]G. G. Kim and K. Char, Bull. Korean Chem. Soc. **20**, 1026 (1999).
[23]C.-M. Chen and Y.-A. Fwu, Phys. Rev. E **63**, 011506 (2000).
[24]J. N. Bright and D. R. M. Williams, Europhys. Lett. **48**, 540 (1999).
[25]D. V. Kuznetsov and Z. Yu. Chen, J. Chem. Phys. **109**, 7017 (1998).
[26]Y. W. Kim, V. Lobaskin, C. Gutsche, F. Kremer, P. Pincus, and R. R. Netz, Macromolecules **42**, 3650 (2009).
[27]F. Yin, D. Bedrov, G. Smith, and S. M. Kilbey II, J. Chem. Phys. **127**, 084910 (2007).
[28]Z. Huang, J. Alonzo, M. Liu, H. Ji, F. Yin, G. D. Smith, J. W. Mays, S. M. Kilbey II, and M. D. Dadmun, Macromolecules **41**, 1745 (2008).
[29]D. Patton, W. Knoll, and R. C. Advincula, Macromol. Chem. Phys. **212**, 485 (2011).
[30]T. T. Pham, S. K. Pattanayek, and G. G. Pereira, J. Chem. Phys. **123**, 034904 (2005).
[31]G. Nam, A. Johner, and N.-K. Lee, J. Chem. Phys. **133**, 164901 (2010).
[32]S. Chandrasekbar, Liq. Cryst. **14**, 3 (1999).
[33]C.-Y. Liu, A. Fechtenkötter, M. D. Watson, K. Müllen, and A. J. Bard, Chem. Mater. **15**, 124 (2003).
[34]D. W. Breiby, F. Hansteen, W. Pisula, O. Bunk, U. Kolb, J. W. Andresen, K. Müllen, and M. M. Nielsen, J. Phys. Chem. B **109**, 22319 (2005).
[35]P. Morales, J. Lagerwall, P. Vacca, S. Laschat, and G. Scatia, Beilstein J. Org. Chem. **6**, 51 (2010).
[36]J. Baschnagel, K. Binder, W. Paul, *et al.*, Adv. Polym. Sci. **152**, 41 (2000).
[37]*Coarse-graining of Condensed Phase and Biomolecular Systems*, edited by G. A. Voth (CRC, Boca Raton, 2009).
[38]D. Reith, A. Milchev, P. Virnau, and K. Binder, EPL **95**, 28003 (2011).
[39]A. Milchev, W. Paul, and K. Binder, J. Chem. Phys. **99**, 4786 (1993).
[40]A. Milchev and K. Binder, Macromol. Theory Simul. **3**, 915 (1994).
[41]A. Milchev and K. Binder, J. Comput.-Aided Mater. Des. **9**, 33 (2002).
[42]D. Deb, A. Winkler, M. H. Yamani, M. Oettel, P. Virnau, and K. Binder, J. Chem. Phys. **134**, 214706 (2011).
[43]M. Müller, Phys. Rev. E **65**, 030802 (2002).
[44]L. Wenning, M. Müller, and K. Binder, Europhys. Lett. **71**, 639 (2005).
[45]*Spin Glasses and Random Fields*, edited by A. P. Young (World Scientific, Singapore, 1988).
[46]K. Binder and W. Kob, *Glassy Materials and Disordered Solids: An Introduction to their Statistical Mechanics* (World Scientific, Singapore, 2011).
[47]M. Doi and S. F. Edwards, *The Theory of Polymer Dynamics* (Clarendon, Oxford, 1986).